VOL. 18, NO. 7, APRIL 2023 ISSN 1819-6608
ARPN Journal of Engineering and Applied Sciences

www.arpnjournals.com

SENSITIVITY OF SUPPORT VECTOR MACHINE TO FEATURES SELECTION FOR LAND COVER CLASSIFICATION BASED ON SENTINEL-2 DATA OVER RIYADH URBAN ARID AREA, SAUDIA ARABIA

Mohammed Saeed, Asmala Ahmad and Othman Mohd.
Faculty of Information and Communication Technology, Universiti Teknikal Malaysia Melaka (UTeM), Durian Tunggal Melaka, Malaysia
E-Mail: P032020006@student.utem.edu.my

ABSTRACT

This study aimed to investigate the effect of three different combinations of features on land cover (LC) classification accuracy with support vector machine (SVM) and Sentinel-2 data over Riyadh city as an urban arid area. The three combinations included the original spectral bands, the spectral indices with spectral bands, and the selected features after applying recursive feature elimination (RFE). The results showed that with constant sample size, adding the spectral indices had a negative influence on SVM performance accuracy metrics. On the other hand, applying RFE as a feature selection improved the accuracy of LC by nearly 2% in the overall accuracy index and by 6% in the f_1-score index. In addition, the feature selection approach decreased the processing time and the number of features for accurate LC classification by removing irrelevant and redundant features. In conclusion, the study showed the importance of applying feature selection with SVM for producing optimal LC classification in the selected urban arid study area.

Keywords: feature selection, land cover, sentinel-2, arid Areas, support vector machine, accuracy.

Manuscript Received 20 February 2023; Revised 18 May 2023; Published 30 May 2023

1. INTRODUCTION

Extracted information from satellite imagery for land cover (LC) and its changes are essential in many applications. This includes urban planning (Hashem & Balakrishnan, 2015), monitoring natural hazards and disasters (Che *et al.*, 2014), desertification monitoring, impact assessment, and environmental studies (Talukdar & Pal, 2020; Nguyen & Liou, 2019).

Adding spectral indices to improve the classification of LC is a common practice in remote sensing communities, such as in Landsat imagery data (Hong *et al*., 2019). Using too many features to improve LC classification requires increasing the training samples size (Huang *et al.*, 2017) to overcome the curse of dimensionality which negatively affects the classification accuracy and increases processing time (Georganos *et al.*, 2018; Gnana *et al*., 2016). Feature selection is very important in LC classification to overcome high-dimensional data to increase class separation and compensate for the limited samples used for training classification models (Huang *et al*., 2017). Moreover, feature selection removes the redundant variables which eventually helps in reducing the training data, and decreasing the processing time (Guyon & Elisseeff, 2003).

According to (Chandrashekar & Sahin, 2014), choosing a feature selection method subject to various considerations such as stability and simplicity. With sentinel-2 imagery, wrapper methods were approved to be more accurate, but with a higher size of selected features (Kiala *et al*., 2019). Despite the several methods which were developed for selecting features, Grenitto *et al.* (Granitto *et al*., 2006) recommended using recursive feature elimination (RFE), a wrapper method, for feature selection due to its stability.

Since Sentinel-2 imagery was released in 2015, it has been widely used in producing LC maps due to its high spatial resolution, and spectral wavelength which helped in distinguishing LC classes (Drusch *et al*., 2012). Different machine-learning classifiers were used to produce LC maps based on Sentinel-2 data imagery in different geographic areas. Support vector machine is one of the most common machine-learning algorithms used for LC classification (Shi & Yang, 2015).

In urban arid areas, the sensitivity of the SVM machine learning classifier to feature selection in terms of LC accuracy has still not been investigated. Therefore, the objective of this study was to explore the effect of the different combinations of features on the accuracy performance of SVM based on Sentinel-2 data imagery with a stable sample size. This included exploring the effect of the RFE feature selection method in selecting the relevant features by applying it to the city of Riyadh as an arid urban area. This will contribute to developing an optimal LC classification SVM model for this study area with the most relevant features, cost-effective samples, and less processing time.

2. MATERIALS AND METHODS

2.1 Study Site and Data

The study area, as shown in Figure-1 was chosen as part of the tile number T38RPN from sentinel-2 satellite imagery that covers the metropolitan city of Riyadh, the capital of Kingdom of Saudia Arabia, as a urban arid area.

The image was selected on 4 July 2022 with ID: L1C_T38RPN_A027817_20220704T073152.

Figure-1. Study area with samples.

Although Sentinel-2 has 13 bands, as shown in Table-1, only 10 bands were used in this study and the 60-meter spatial resolution bands related to atmospheric and cloud detection were removed.

Table-1. Spectral bands in Sentinel-2 data.

Band	Resolution (m)	Central Wavelength (nm)
b1	60	443
b2	10	490
b3	10	560
b4	10	665
b5	20	705
b6	20	740
b7	20	783
b8	10	842
b8a	20	865
b9	60	945
b10	60	375
b11	20	610
b12	20	190

2.2 Data Preprocessing and Preparation

To standardize the spatial resolution and achieve optimal accuracy, the 20-meter spatial resolution bands (Table-1) were downscaled to 10 meters using the nearest neighbor technique which was approved to be more accurate than other techniques in terms of producing LC classification maps (Zheng *et al*., 2017). After that, the image was cropped to the study area shapefile using QGIS software, version 3.

2.3 Training and Testing Samples

The selection of LC classes was based on the idea which confirms the inclusion of the mainland types in the study area concerning previous studies (Alqurashi et al., 2016; Rahman & Planning, 2016). In this study, the urban class has been divided into three categories: roads, industrial, and buildings where spectral differences are unique. Figure-2 shows the classes with their training and testing samples number.

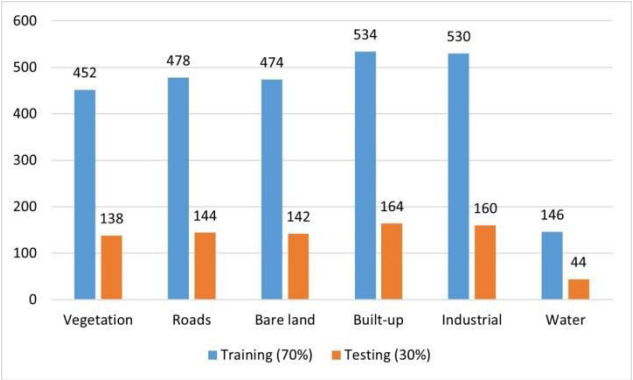

Figure-2. Land cover classes with their training and testing numbers.

The stratified random sampling method was used to collect training and testing samples. All samples were collected based on a single pixel as a classification unit taking into consideration the effect of spatial autocorrelation. Choosing samples was based on visual interpretation of the high spatial resolution Google Earth maps with intensive fieldwork for validation. The number of training samples was determined to be in the range of 10–30 times the number of bands used for classification (Li *et al.,* 2014). The test samples were 30% of the total samples and independent of the training samples.

2.4 Classification Process and Evaluation

To investigate the effect of the different combinations of features on LC classification accuracy performance in this study area, we compared the performance of SVM with three different combinations of features. The first combination consisted of the original ten spectral bands already mentioned in Table-1. The second combination used the same features of the first combination in addition to five common spectral indices, namely: the normalized difference vegetation index (NDVI), the normalized difference built-up index (NDBI), the modified normalized difference water index (MNDWI), the bare soil index (BSI), and the soil adjusted vegetation index (SAVI). These spectral indices are commonly used as ancillary features to improve LC

accuracy. The third combination represents the selected features that achieved the best performance accuracy metrics after applying RFE as a feature selection technique.

In each combination, the accuracy performance of SVM during the model training process was validated using a 10-fold cross-validation technique to avoid bias in results and conclusions. In this technique, the data set is divided into 10 subsets. Next, a model is trained using a subset formed by combining these nine subsets and tested using the remaining subset. This is done 10 times each using a different subset as a test set and calculating the test set error.

The SVM evaluation for all feature combinations was based on the performance metrics represented by the overall accuracy (OA), the user's (UA), and the producer's (PA) accuracies which were calculated from the confusion matrix. In addition, the f_1-score was calculated as a balance accuracy measurement (Richard *et al*., 2017) and used in this study as the main index for comparing the models.

The last step of the evaluation was the computational time analysis which included comparing the processing time for the three combinations with their different number of features. The average of 10 running times was used in this study for the processing time of the model during training and when the models were used to predict the whole image of the study area. All analyses were carried out using R programming language (version 3.6.1). We used a laptop with Intel® CoreTM i7-7700HQ CPU @ 2.80GHz × 8 and 32 GiB memory in Ubuntu 20.04.5 LTS operating system.

3. RESULTS

3.1 Accuracy Assessment

3.1.1 SVM Performance with spectral bands

Table-2 shows the confusion matrix when the classification model used only the tenth spectral band. The OA of the model was 83.08 %. Generally speaking, the most misclassification appeared between vegetation and built-up classes on one hand and between industrial and bare classes on the other hand.

Table-2. Confusion matrix of the SVM model_1.

		Predicted values						
	Classes	**Vegetation**	**Roads**	**Bare land**	**Built-up**	**Industrial**	**Water**	**Total**
Actual values	Vegetation	102	2	2	32	0	0	138
	Roads	0	134	0	10	0	0	144
	Bare land	0	0	138	0	4	0	142
	Built-up	2	2	4	156	0	0	164
	Industrial	0	0	30	4	126	0	160
	Water	4	6	0	32	0	2	44
	Total	108	144	174	234	130	2	792
		Overall accuracy 83.08%						

In this model and as shown in FIGURE-3, the PA, and UA vary in values among the classes. The PA for the bare land class was the maximum at 97.2%, while the water class had the minimum value at 4.5 percent. Regarding the UA, the water and built-up classes were the highest and lowest values with 100 and 66.7 respectively.

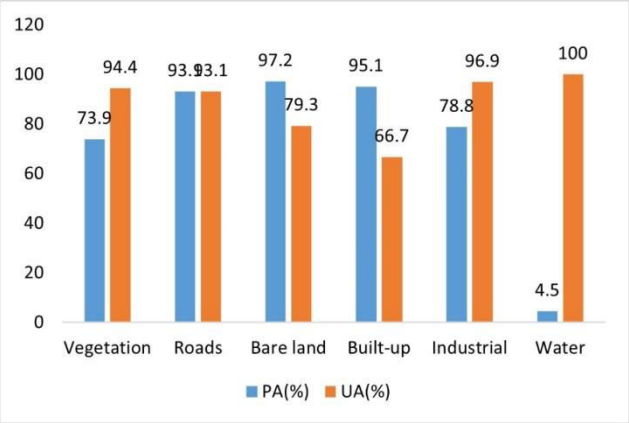

Figure-3. The user's (UA) and producer (PA) accuracies in SVM model_1.

In this model, as shown in Figure-4, the f_1-score has different values among the sex classes. The roads class got the highest score with 93.06 %, while the water class got the lowest accuracy value with 8.7 %.

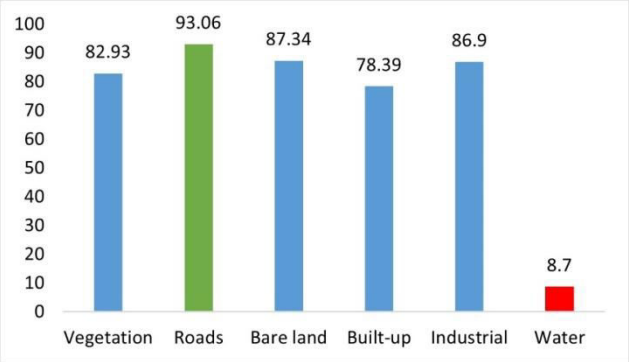

Figure-4. F_1-score accuracy in SVM model_1.

3.1.2 SVM Performance with spectral bands and spectral indices

Table-3 shows the confusion matrix when the classification model used the tenth spectral band with the five spectral indices. The OA of this model decreased by 0.76 % compared to the previous model.

Table-3. Confusion matrix of the SVM model_2.

		Predicted values						
	Classes	**Vegetation**	**Roads**	**Bare land**	**Built-up**	**Industrial**	**Water**	**Total**
Actual values	Vegetation	94	2	2	40	0	0	138
	Roads	2	132	0	10	0	0	144
	Bare land	0	0	138	0	4	0	142
	Built-up	2	2	2	158	0	0	164
	Industrial	0	0	34	0	126	0	160
	Water	6	10	0	24	0	4	44
	Total	104	146	176	232	130	4	792
		Overall accuracy 82.32 %						

This per-class decrease in accuracy is shown in Figure-5 where it is very clear that the decrease occurred in vegetation, and roads in 8 and 2 instances respectively. The bare and industrial classes did not experience any change and were constant in both models. On the other hand, there was a relative increase in the accuracy of the built-up and water classes by 2 instances for both of the two classes respectively.

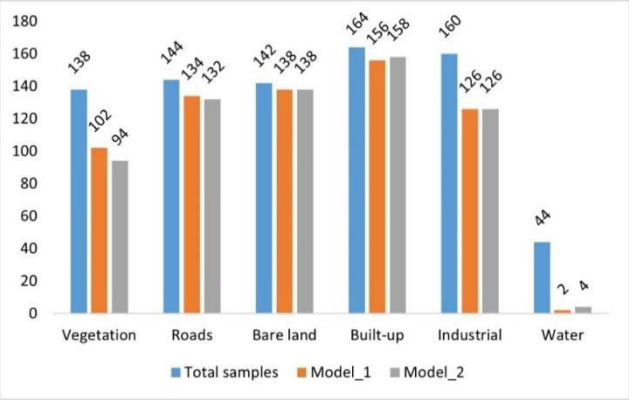

Figure-5. Comparison of correctly classified instances in the SVM model_2.

As shown in fig Figure-6, the PA and UA accuracy in this model are variated. The highest and lowest PA values were registered for the bare land and water classes by 97.2 and 9.1 percent respectively, while

the highest and lowest UA values were registered for water and industrial classes by 100 and 96.9 percent respectively.

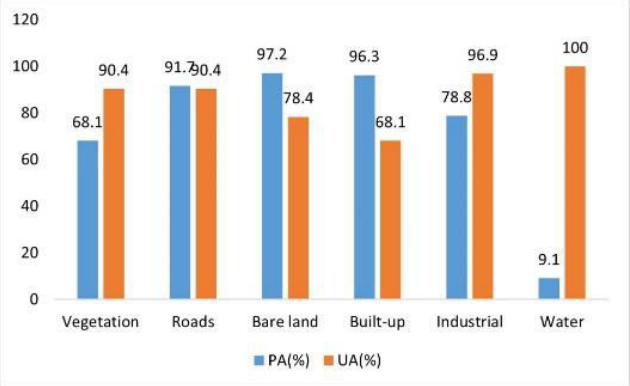

Figure-6. The user's (UA) and producer (PA) accuracies in SVM model_2.

In this model, as shown in Figure-7, the f_1-score has different values among the sex classes. The road class got the highest score of 91.03 %, while the water class got the lowest accuracy value of 16.67 %.

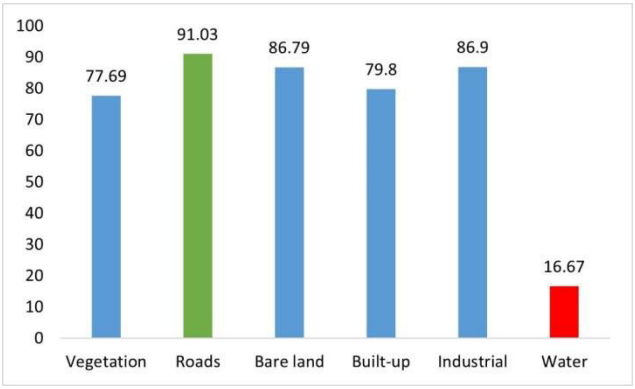

Figure-7. F_1-score accuracy in SVM model_2.

3.1.3 SVM Performance with RFE feature selection method

The confusion matrix after applying the RFE to subset the feature with the best accuracy is shown in TABLE-4 Confusion matrix of the SVM model_3. The best accuracy derived from this model was 85.35 % using only eight features: six spectral bands: b2, b3, b6, b8, b8A, and b12 with two spectral indices: MNDWI and BSI. Comparing this model with the previous two models: model_2 and model_1, the OA accuracy in this model increased by 3.03%, and 2.27 % respectively.

Table-4. Confusion matrix of the SVM model_3.

		Predicted values						
	Classes	**Vegetation**	**Roads**	**Bare land**	**Built-up**	**Industrial**	**Water**	**Total**
Actual values	Vegetation	88	38	2	8	0	2	138
	Roads	4	134	0	6	0	0	144
	Bare land	0	0	136	0	6	0	142
	Built-up	4	6	0	154	0	0	164
	Industrial	0	0	8	0	152	0	160
	Water	2	14	0	16	0	12	44
	Total	98	192	146	184	158	14	792
Overall accuracy 85.35 %								

The majority of accuracy improvement was in both industrial and water classes where the number of the correct instances increased by 26 and 8 respectively in comparison with the same classes in the previous model_2 as shown in Figure-8.

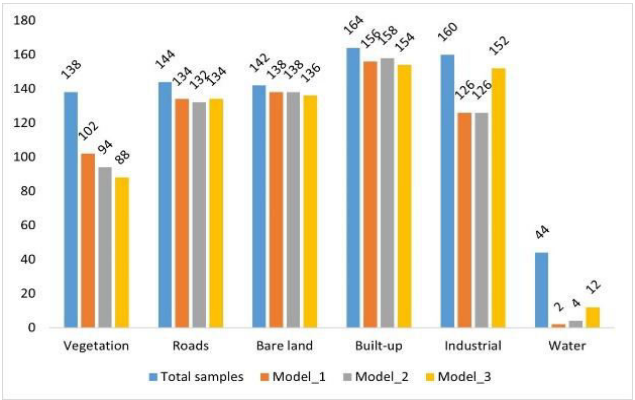

Figure-8. Comparison of correctly classified instances in SVM models.

In this model, as shown in Figure-9, the PA ranged between 27.3 % for the water class and 95.8 % for the bare land class. In terms of the UA, the water class ranked the best with 96.2 %, while the road class ranked the lowest with 69.8 %.

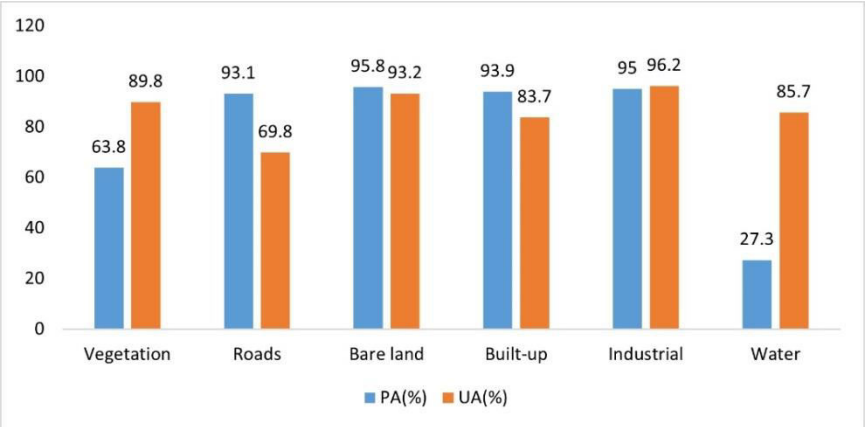

Figure-9. The user's (UA) and producer's (PA) accuracies in SVM model_3.

In this model, as shown in Figure-10, the f_1-score has different values among the sex classes. The industrial class got the highest score 95.6 %, while the water class got the lowest accuracy value 41.38 %.

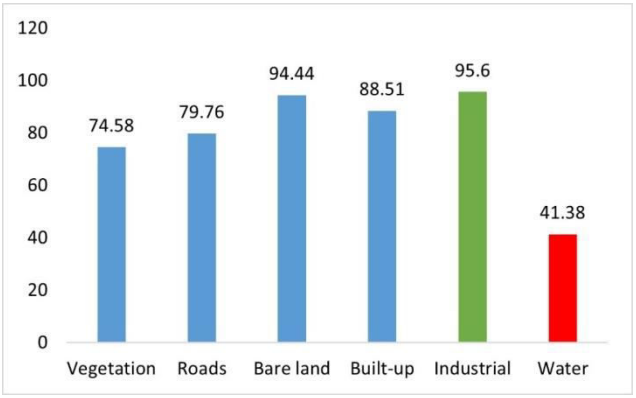

Figure-10. F_1-score accuracy in SVM model_3.

From the previous three combinations in the SVM model, the per-class accuracy instances were different from one model to another. By referring to Figure-8, model_1 achieved a higher number of the correct vegetation class instances by 102 out of 138. Model_2 gained the best number of correctly classified instances for built-up by 158 instances out of 164, while model_3 achieved the best results for industrial and water classes by 152 and 12 instances out of 160 and 44 for each class respectively.

For the class of the road, the correct number of instances was equally achieved by 134 instances in model_1 and model_3. In the bare-land class, Model_1 and model_2 got equally the best number of correctly classified instances 138 out of 142. The worst performance in the number of correctly classified instances was documented for the water class where only 2, 4, and 12 instances were achieved by model_1, model_2, and model_3 respectively.

In terms of the OA, average PA, UA, and f_1-score as shown in Figure-11, model_3 achieved the best score with 85.35 %, 78.15 %, and 79.15 % for OA, average PA, and f_1 respectively. Most of the accuracy metrics were decreased in model_2 after adding the spectral indices to the spectral bands. On the other hand, in model_3, there was a noticeable increase in the accuracy of all these metrics after applying the RFE feature selection technique. In conclusion, model_3 represents the best choice achieved by the SVM classifier according to the accuracy metrics.

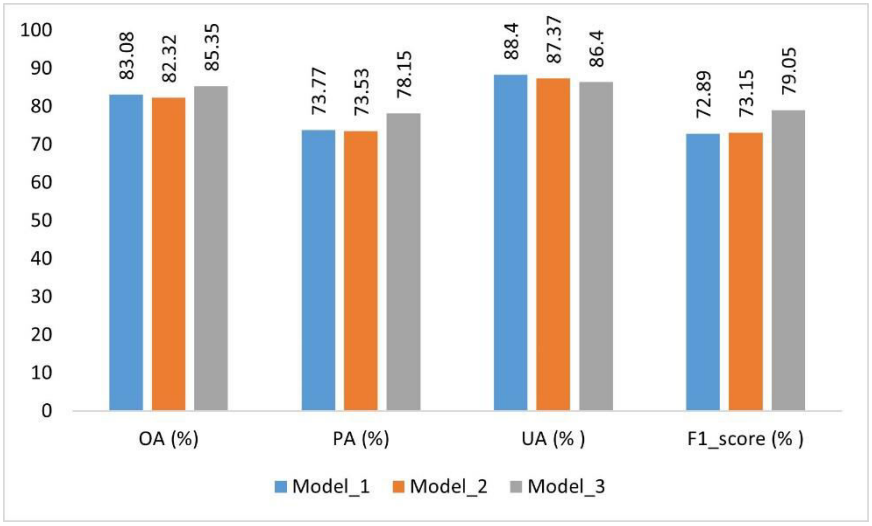

Figure-11. Average accuracy indicators for the three SVM models.

3.2 Computation Time

In this study, as shown in FIGURE-12, the processing time consumed for the three combinations of features was variated. In combination 1, training and prediction processing time were 2.21 and 2.17 minutes respectively. These values were increased in combination 2 to reach 2.57 and 2.51 minutes for both of training and prediction processing time respectively. In combination 3, training and prediction processing time were 2.08 and 1.97 minutes respectively.

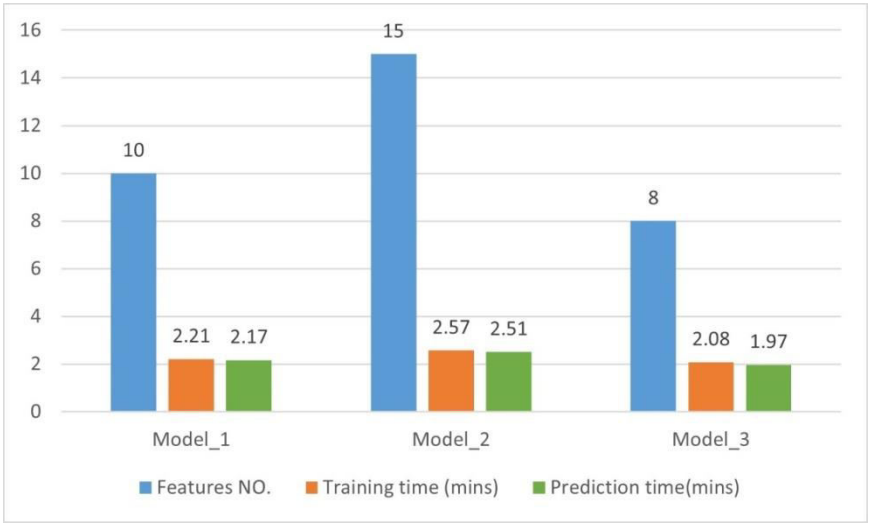

Figure-12. Average processing time with features number in the three models.

Processing time in the three combinations was affected by the number of features used, where less processing time was associated with the lowest number of features (combination 3) and vice versa.

4. DISCUSSIONS

In this study, after adding the spectral indices in model_2, there was a decrease in OA and too little improvement in f_1-score accuracy performance. These findings are different from various studies [5], [27], [28] which proved the efficiency of the spectral indices in improving the LULC classification. These contradictory results can be attributed to the cursor of multidimensionality. The number of training samples in this study was constant in the three combinations and limited to 15 times the total number of features, thus adding the new spectral indices in model_2 increased the predictive features without increasing the training samples leading to the appearance of the cursor of dimensionality through the decrease in performance accuracy metrics and increasing the processing time (Löw *et al.*, 2013). According to (Huang *et al.,* 2017), increasing the number of features should be associated with increasing the training samples to avoid the effect of the cursor of dimensionality.

Applying RFE in this study showed decreasing the predictive variables and reduced the processing time as shown in model_3. In addition, an improvement in OA and f_1-score accuracy performance was documented. The application of feature selection for improving LC

classification in this study was aligned with results from other studies. (Stromann et al., 2019) showed that applying feature selection improved LC classification in two urban areas. In an urban area, (Doğan & Uysal, 2018) showed that all the feature selection methods were effective in improving the LULC classification with different percentages.

The feature selection techniques help in dimensionality reduction and speeding the process. This finally removes the redundant and irrelevant data which indirectly improves the accuracy (Löw *et al*., 2013). In this study, RFE decreased the predictive features to nearly half in most cases and also decreased both training and prediction processing time with all the classifiers.

In terms of the processing time, findings in this study refer in general that the processing time showed an increasing trend when models only used the spectral bands (model_1) in comparison with the combination of the spectral bands and indices(model_2). In addition, a decreased trend in computation time after applying RFE (model_3) in comparison with model_2. Furthermore, the classifier's training processing time was lower than the processing time during the classifier's prediction. These results are in agreement with the study conducted by (Ramezan *et al*., 2021) and *(Rumora et al.*, 2020) which showed that the trend in speed is attributed to the number of features and the amount of sample size during the training and prediction process of the classifier.

5. CONCLUSIONS

In this study, the SVM accuracy performance analysis was investigated using three different combinations of features including the original spectral bands of Sentinel-2 data, the original bands with five common spectral indices, and the features resulting from the two combinations after applying the RFE method. The accuracy performance metrics were compared in the three combinations using the same sample size.

The results showed that improving LC accuracy by adding the spectral indices is not effective in comparison with using only the original spectral bands with the same sample size where the OA accuracy was decreased from 83.08% to 82.32 % and the average f_1-score was slightly improved by only 0.26%. in addition, the training and prediction processing time was increased by 0.36 and 0.34 minutes respectively.

In contrast, applying RFE in combination 3 was so effective in improving LC accuracy and processing time where the OA was improved by 2.27% and 3.03% in comparison with combination 2 and combination 1 respectively. In addition, the average f_1-score in this combination was increased by 5.9% and 6.16% in comparison with the same accuracy performance metrics in combination 2 and combination 1 respectively. Furthermore, only 8 features were used for this improvement in comparison with 15 and 10 features in combination 2 and combination 1. Consequently, the training and prediction processing time was decreased in this combination by 0.49 and 0.54 minutes in comparison with the time consumed in combination 2 and by 0.13 and 0.2 minutes in comparison with the time consumed in combination 1.

For generalization and improving the accuracy of LC in urban arid areas, the other classifiers with different feature selection methods can be investigated and compared in the context of optimization of the LC classification process and hardware resources requirements.

REFERENCES

Abdi A. M. 2020. Land cover and land use classification performance of machine learning algorithms in a boreal landscapeusing Sentinel-2 data. GIScience & Remote Sensing, 57(1).

Alqurashi A. F., Kumar L. and Sinha P. 2016. Urban land cover change modelling using time-series satellite images: A case study of urban growth in five cities of Saudi Arabia. Remote Sensing. 8(10): 838.

Campos J. C., Sillero N. and Brito, J. C. 2012. Normalized difference water indexes have dissimilar performances in detecting seasonal and permanent water in the Sahara-Sahel transition zone. Journal of Hydrology. 464, 438-446.

Chandrashekar G. and Sahin F. 2014. A survey on feature selection methods. Computers & Electrical Engineering. 40(1): 16-28.

Che T., Xiao L. and Liou Y.-A. 2014. Changes in glaciers and glacial lakes and the identification of dangerous glacial lakes in the Pumqu River Basin, Xizang (Tibet). Advances in Meteorology.

Dao P. D. and Liou Y.-A. 2015. Object-based flood mapping and affected rice field estimation with Landsat 8 OLI and MODIS data. Remote Sensing. 7(5): 5077-5097.

Doğan T. and Uysal K. A. 2018. The impact of feature selection on urban land cover classification.

Drusch M., Del Bello U., Carlier S., Colin O., Fernandez V., Gascon F., Hoersch B., Isola C., Laberinti P. and Martimort P. 2012. Sentinel-2: ESA's optical high-resolution mission for GMES operational services. Remote Sensing of Environment. 120, 25-36.

Ge G., Shi Z., Zhu Y., Yang X. and Hao Y. 2020. Land use/cover classification in an arid desert-oasis mosaic landscape of China using remote sensed imagery: Performance assessment of four machine learning algorithms. Global Ecology and Conservation, 22, e00971. https://doi.org/10.1016/j.gecco.2020.e00971

Georganos S., Grippa T., Vanhuysse S., Lennert M., Shimoni M., Kalogirou S. and Wolff E. 2018. Less is more: Optimizing classification performance through feature selection in a very-high-resolution remote sensing

object-based urban application. GIScience & Remote Sensing. 55(2): 221-242.

Gnana D. A. A., Balamurugan S. A. A. and Leavline E. J. 2016. Literature review on feature selection methods for high-dimensional data. International Journal of Computer Applications. 136(1): 9-17.

Granitto P. M., Furlanello C., Biasioli F. and Gasperi F. 2006. Recursive feature elimination with random forest for PTR-MS analysis of agro industrial products. Chemometrics and Intelligent Laboratory Systems. 83(2): 83-90.

Guyon I. and Elisseeff A. 2003. An introduction to variable and feature selection. The Journal of Machine Learning Research. 3(null): 1157-1182.

Hashem N. and Balakrishnan P. 2015. Change analysis of land use/land cover and modelling urban growth in Greater Doha, Qatar. Annals of GIS. 21(3): 233-247.

Hong C., Jin X., Ren J., Gu Z. and Zhou Y. 2019. Satellite data indicates multidimensional variation of agricultural production in land consolidation area. Science of the Total Environment. 653, 735-747.

Huang Y., Zhao C., Yang H., Song X., Chen J. and Li Z. 2017. Feature selection solution with high dimensionality and low-sample size for land cover classification in object-based image analysis. Remote Sensing. 9(9): 939.

Kiala Z., Mutanga O., Odindi J. and Peerbhay K. 2019a. Feature selection on sentinel-2 multispectral imagery for mapping a landscape infested by parthenium weed. Remote Sensing. 11(16): 1892.

Kiala Z., Mutanga O., Odindi J. and Peerbhay K. 2019b. Feature selection on sentinel-2 multispectral imagery for mapping a landscape infested by parthenium weed. Remote Sensing. 11(16): 1892.

Li C., Wang J., Wang L., Hu L. and Gong P. 2014. Comparison of classification algorithms and training sample sizes in urban land classification with Landsat thematic mapper imagery. Remote Sensing. 6(2): 964-983.

Liou Y.-A., Kar S. K. and Chang L. 2010. Use of high-resolution FORMOSAT-2 satellite images for post-earthquake disaster assessment: A study following the 12 May 2008 Wenchuan Earthquake. International Journal of Remote Sensing. 31(13): 3355-3368.

Liou Y.-A., Nguyen A. K. and Li M.-H. 2017. Assessing spatiotemporal eco-environmental vulnerability by Landsat data. Ecological Indicators. 80, 52-65.

Liou Y.-A., Sha H.-C., Chen T.-M., Wang T.-S., Li Y.-T., Lai Y.-C. and Chiang M.-H. 2012. Assessment of disaster losses in rice paddy field and yield after Tsunami induced by the 2011 great east Japan earthquake. Journal of Marine Science and Technology. 20(6): 2.

Loukika K. N., Keesara V. R. and Sridhar V. 2021. Analysis of land use and land cover using machine learning algorithms on google earth engine for Munneru River Basin, India. Sustainability. 13(24): 13758.

Löw F., Michel U., Dech S. and Conrad C. 2013. Impact of feature selection on the accuracy and spatial uncertainty of per-field crop classification using support vector machines. ISPRS Journal of Photogrammetry and Remote Sensing. 85, 102-119.

Nguyen K.-A. and Liou Y.A. 2019. Global mapping of eco-environmental vulnerability from human and nature disturbances. Science of the Total Environment. 664, 995-1004.

Pal M. and Foody G. M. 2010. Feature selection for classification of hyperspectral data by SVM. IEEE Transactions on Geoscience and Remote Sensing. 48(5): 2297-2307.

Rahman M. and Planning R. 2016. Land use and land cover changes and urban sprawl in Riyadh, Saudi Arabia: An analysis using multi-temporal Landsat data and Shannon's Entropy Index. The International Archives of the Photogrammetry, Remote Sensing and Spatial Information Sciences. 41, 1017-1021.

Ramezan C. A., Warner T. A., Maxwell A. E. and Price B. S. 2021. Effects of training set size on supervised machine-learning land-cover classification of large-area high-resolution remotely sensed data. Remote Sensing. 13(3): 368.

Richard K., Abdel-Rahman E. M., Subramanian S., Nyasani J. O., Thiel M., Jozani H., Borgemeister C. and Landmann T. 2017. Maize cropping systems mapping using rapideye observations in agro-ecological landscapes in Kenya. Sensors. 17(11): 2537.

Rumora L., Miler M. and Medak D. 2020. Impact of various atmospheric corrections on Sentinel-2 land cover classification accuracy using machine learning classifiers. ISPRS International Journal of Geo-Information. 9(4): Article 4.

Shi D. and Yang X. 2015. Support vector machines for land cover mapping from remote sensor imagery. In Monitoring and Modeling of Global Changes: A Geomatics Perspective (pp. 265-279). Springer.

Stromann O., Nascetti A., Yousif O. and Ban Y. 2019. Dimensionality reduction and feature selection for object-based land cover classification based on Sentinel-1 and Sentinel-2 time series using Google Earth Engine. Remote Sensing. 12(1): 76.

Talukdar S. and Pal S. 2019. Effects of damming on the hydrological regime of Punarbhaba river basin wetlands. Ecological Engineering. 135, 61-74.

Talukdar S. and Pal S. 2020. Wetland habitat vulnerability of lower Punarbhaba river basin of the uplifted Barind region of Indo-Bangladesh. Geocarto International. 35(8): 857–886.

Van Niel T. G., McVicar T. R. and Datt B. 2005. On the relationship between training sample size and data dimensionality: Monte Carlo analysis of broadband multi-temporal classification. Remote Sensing of Environment. 98(4): 468-480.

Zheng H., Du P., Chen J., Xia J., Li E., Xu Z., Li X. and Yokoya N. 2017. Performance evaluation of downscaling Sentinel-2 imagery for land use and land cover classification by spectral-spatial features. Remote Sensing. 9(12): 1274.